The In-situ Mechanical Testing of Nanoscale Single-crystalline Nanopillars

Julia R. Greer, Ju-Young Kim, and Michael J. Burek

This article reviews recent studies on the mechanical properties of cylindrical metallic nanopillars subjected to uniaxial deformation. Remarkable strengths and very different mechanical properties arise due to the activation of unique deformation mechanisms operating in these nanoscale volumes. Effects of both size and microstructure are discussed.

INTRODUCTION

Beyond classical strengthening methodologies utilized by engineers for centuries, it was recently shown that at the micrometer and sub-micrometer scales, sample size can dramatically increase crystalline strength, as revealed by room-temperature uniaxial compression experiments on a wide range of single-crystalline metallic nanopillars with non-zero initial dislocation densities. In these studies, cylindrical nanopillars were fabricated by focused ion beam (FIB) and, remarkably, the results of all of these reports indicate a power-law dependence between the flow stress and sample size, implying that this scaling might be universal. On the other hand, the classical copper wire tension experiments performed by Brenner et al. in the 1950s, as well as a few recent works indicate that when the FIB is not involved in the sample fabrication, similar-sized features in some of the same metals attain close-to-theoretical strengths with no observed size effects. The sample fabrication methods used in these studies, however, result in a pristine microstructure, with no initial defects, allowing the material to attain ideal strengths. Therefore, there are some deeper outstanding questions, with the main one being: to what extent is the size effect in metals, which manifests itself as "smaller is stronger" for single crystals, driven by the sample size vs. by the initial microstructure. Understanding plastic response in single crystals provides a solid foundation for identifying deformation mechanisms operating in more complex material systems, the knowledge of which is essential for the creation and property control of new, revolutionary materials.

How would you…

…describe the overall significance of this paper?

This article offers a review of some of the latest advances in ex- and in-situ nanoscale mechanical testing of single crystals, which have been found to exhibit significantly higher strengths when their dimensions are reduced to the sub-micrometer scale.

…describe this work to a materials science and engineering professional with no experience in your technical specialty?

Uniaxial deformation of nanoscale metallic nanopillars offer a powerful platform to study mechanical properties of materials in small volumes. It is no longer feasible to infer the bulk values of these materials from literature since they have been found to significantly deviate from bulk and need to be assessed at the appropriate scale.

…describe this work to a layperson?

Common materials like metals appear to have unique and interesting properties when reduced to nanoscale. One example is that they become significantly stronger, exhibiting strengths an order of magnitude higher than bulk. Understanding material strength at the appropriate scale is crucial in the design and reliable functioning of devices comprised of these materials.

SIZE EFFECTS IN CRYSTALLINE PLASTICITY

Until recently, mechanical deformation has largely been carried out in thin films on stiff substrates—for example, silicon, sapphire, and MgO—via nanoindentation, in which a sharp diamond tip is applied into the material and the load on the indenter tip is measured as a function of its displacement into the surface.[1] Some of the mechanisms responsible for strengthening in thin films are well understood and can be attributed to grain size hardening,[2] the confinement of dislocations within the film by the substrate,[3] or the presence of strong strain gradients.[4] Where strain gradients are present (i.e., nanoindentation), the size effect in single crystals is commonly attributed to the density of so-called geometrically necessary dislocations (GNDs), which form to accommodate the permanent shape change. The relationship between GNDs and the plastic strain gradient is the key concept behind many strain-gradient plasticity theories.[5–11] These size effects arise from the constraining effects of the surrounding layers, from inhomogeneity of the deformation, or from specific microstructures present in these thin films. Unlike these "extrinsic" size effects, a significant increase in strength has recently been reported when single crystals are deformed in small, unconstrained volumes. To study mechanical deformation of crystals in small volumes without introducing strain gradients, Uchic et al.[12] developed a uniaxial compression methodology for FIB-machined nickel-based alloys via a modification of the nanoindentation technique. Building on this methodology, Greer and Nix were first to extend this type of experiment into the na-

noscale regime, where they discovered very different plasticity mechanisms operating in single-crystalline gold nanopillars with diameters below 1 μm. Influenced by this testing methodology, several groups explored size effects in plasticity by investigating mechanical behavior of single-crystalline micropillars. In these studies, uniaxial compression tests were performed on Ni and Ni-based superalloys,[12–14] Au,[15–18] Cu,[19] Mo,[20,21] and Al[22] micro- and nanopillars having diameters from 100 nm to tens of micrometers, with aspect ratio (length/diameter) in the range between 2:1 and 5:1. These experiments revealed a remarkable dependence of the attained flow strength on the diameter, most likely due to the presence of unique deformation mechanisms in plasticity at nanoscale (see Figure 1).[23] The results of these studies convincingly showed that the yield and flow stresses increase significantly with reduced size, with the smallest specimens of ~200 nm sometimes attaining a flow stress an order of magnitude higher than bulk materials.[1,15–17,23,24] Another common observation in these types of experiments is that unlike Taylor hardening, the flow strength does not appear to scale with the evolving dislocation density. While compression experiments are gaining momentum, performing tensile experiments has been much more challenging since it requires a custom-made in-situ mechanical deformation system, and only a few groups in the world are capable of doing it. Recently, Kiener et al. reported a new method to measure tensile behavior of single crystals at the micro- and nanoscales,[25] in which tension samples were fabricated using an FIB, and uniaxial tensile testing was performed inside a scanning electron microscope (SEM) and a transmission electron microscope (TEM).[26] These authors also reported the presence of a size effect, albeit less pronounced than in compression, and found it to be strongly dependent on the aspect ratio of the sample.[27] Size-dependent hardening was attributed to the formation of dislocation pile-ups due to the constrained glide of the dislocations in the sample caused by the sample geometry and gripping constraints. This team of authors has also done extensive work on investigating the effects of experimental constraints—both due to sample geometry and the loading mechanism—during micro-compression and tension experiments.[27–29] In our recent work, we have examined size effects in tension vs. compression of two types of crystals: gold (face-centered cubic, f.c.c.) and molybdenum (body-centered cubic, b.c.c.) and found that in the former the size dependence between the two loading directions is identical while in the latter, there is a pronounced tension-compression asymmetry.[30]

One notable exception to the compression studies is the work of Bei et al.[20] who observed no size effects in uniaxial compression of molybdenum alloy micro-columns prepared by chemically etching away the matrix of a directionally solidified NiAl-Mo eutectic, which attained theoretical strength regardless of the sample size. Beyond the classical work of Brenner et al.,[31] who demonstrated the attainment of theoretical strength in copper, iron, and silver micro-wires subjected to uniaxial tension, the lack of size effects was also observed by Richter et al.[32] who grew pristine (i.e., defect-free) single-crystalline copper nano-whiskers and

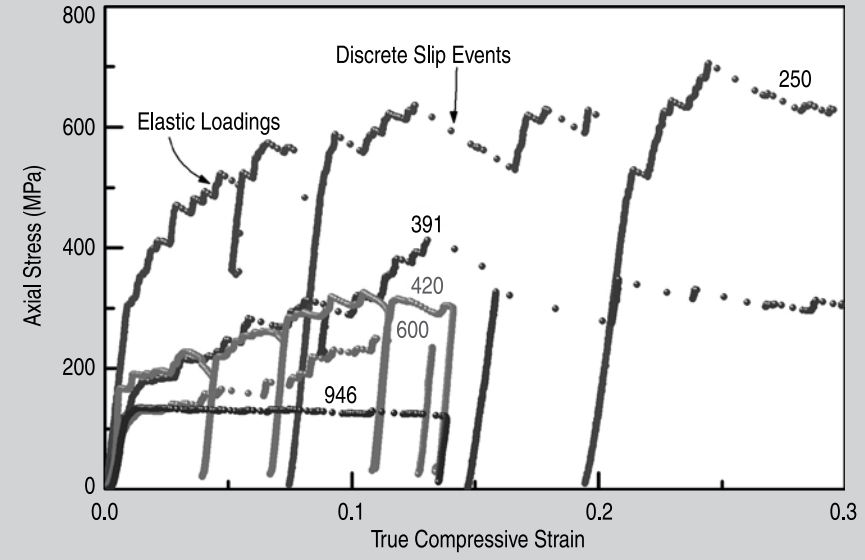

Figure 1. Representative stress-strain curves for compression of <001>-oriented gold nanopillars; the numbers above each curve correspond to the pillar diameter. This plot clearly shows the "smaller is stronger" phenomenon (graph is taken from Reference 23).

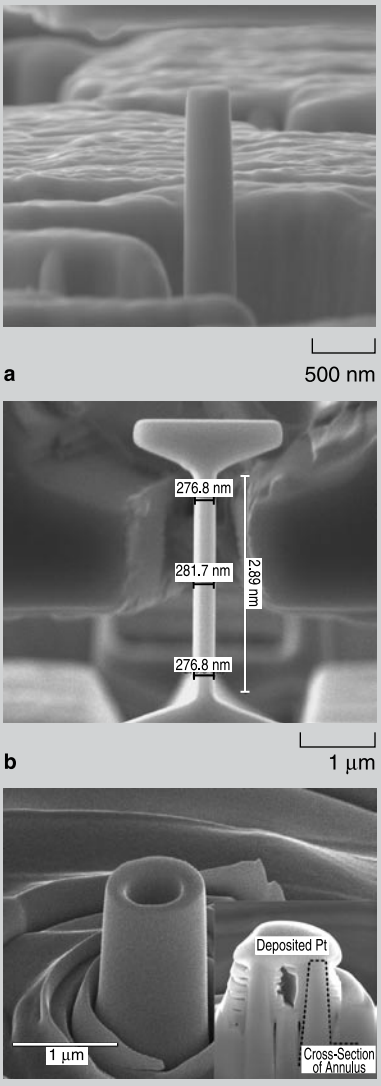

Figure 2. Scanning electron microscopy images of mechanical testing samples of different materials, geometries, and sizes. (a) Nanocrystalline nickel pillar with grain size of 60 nm, (b) 200-nm diameter single-crystal niobium tension sample, (c) molybdenum annulus with inset showing platinum traces to identify inner wall shape.

demonstrated their fracture strength to be close to the theoretical limit. All of these studies employed sample fabrication methods that resulted in the creation of virtually defect-free initial microstructure, rendering the attainment of theoretical strength not surprising. An interesting feature of these and some other works,[33,34] however, is that intentional introduction of dislocation into the structure by pre-straining weakens these crystals, a finding in stark contrast to that of classical plasticity where dislocation multiplication is the very mechanism responsible for work-hardening. These findings convincingly suggest that besides the crystal dimensions, a key parameter that might contribute to the size effect is the initial dislocation density in single crystals.

COMPUTATIONAL RESULTS

As we discover more about the influence of sample size on the stress-strain response, another distinction has recently been reported; namely, different crystal structures appear to undergo fundamentally different plasticity mechanisms in uniaxial compression. Greer et al.[35] and Brinckmann et al.[23] showed that there is a significant difference in scaling slopes as well as in the fraction of the attained ideal strength between gold (f.c.c.) and molybdenum (b.c.c.) crystals. Recent work of Weinberger and Cai using Parallel Dislocation Simulation (ParaDis), dislocation dynamics (DD), and molecular dynamics (MD) simulations revealed that this difference is likely due to the distinct differences in dislocation loop behavior inside of b.c.c. vs. f.c.c. pillars.[36] Due to a significant controversy in the phenomenological explanations for the higher strengths attained by sub-micrometer sized pillars subjected to uniaxial deformation, atomistic computer simulations have been utilized as a means to provide useful insights in understanding the origins of deformation mechanisms responsible for the observed size effect. For example, a number of two- and three-dimensional DD simulations have been performed. Deshpande et al.[37] conducted two-dimensional (2-D) compression and tension DD simulations of planar single crystal slabs by incorporating a number of constitutive rules and allowing two extreme cases of boundary conditions for tensile axis rotation: fully constrained or allowed to rotate. Based on the small-strain analysis, they reported a power-law strength vs. size dependence with a somewhat lower exponent than experimentally observed at the time. Using a similar approach, Benzerga and Shaver[38] incorporated dislocation nucleation length and time as model parameters and concluded that the apparent strengthening is due to the generation of internal stresses and to the dislocation source length variation. Building upon this work, Guruprasad and Benzerga[39] effectively created "2.5-D" simulations

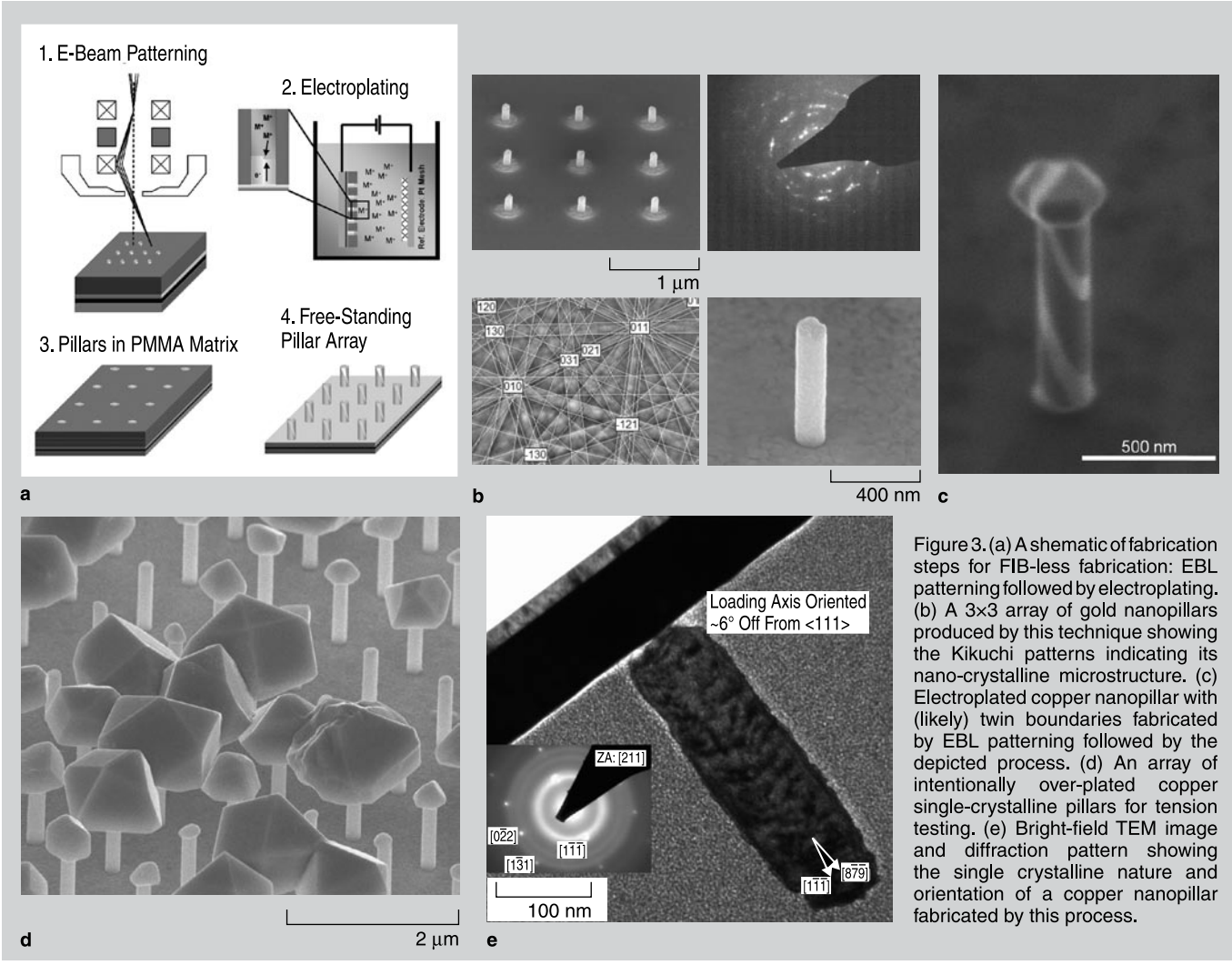

Figure 3. (a) A shematic of fabrication steps for FIB-less fabrication: EBL patterning followed by electroplating. (b) A 3×3 array of gold nanopillars produced by this technique showing the Kikuchi patterns indicating its nano-crystalline microstructure. (c) Electroplated copper nanopillar with (likely) twin boundaries fabricated by EBL patterning followed by the depicted process. (d) An array of intentionally over-plated copper single-crystalline pillars for tension testing. (e) Bright-field TEM image and diffraction pattern showing the single crystalline nature and orientation of a copper nanopillar fabricated by this process.

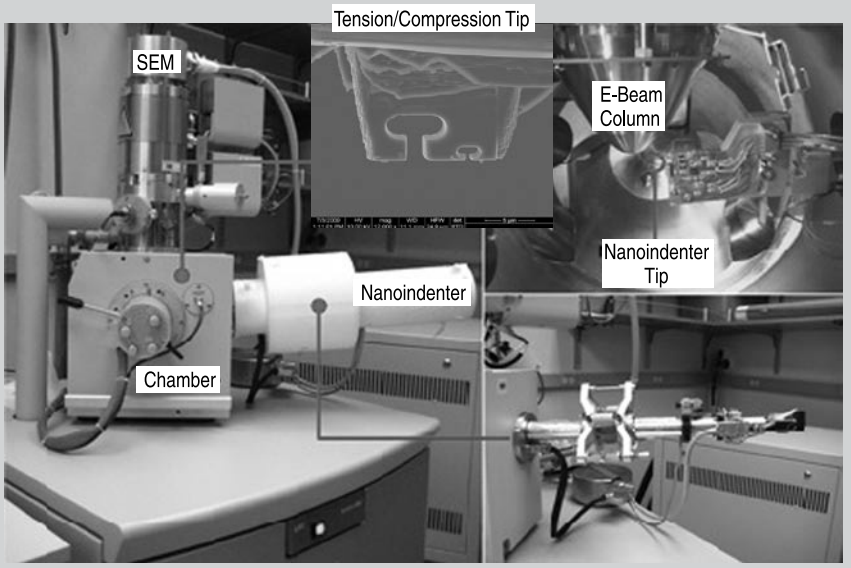

Figure 4. SEMentor—the custom in-situ mechanical testing instrument built in our lab comprised of SEM and nanoindenter. The inset shows tension-compression mechanical testing grips as fabricated by FIB from a standard Berkovich indenter tip.

for high-initial-dislocation-density nanoscale f.c.c. crystals and showed that even at such high densities Taylor hardening does not hold. They proposed that the increased hardening rate of smaller specimens is mainly due to the creation of the localized internal strain gradients even during homogeneous deformation. While 2-D DD simulations provide useful insight into nanoscale plasticity, they are not capable of capturing the effects of cross-slip, dislocation line tension, and ad-hoc dislocation interactions, which are key in crystalline plasticity. The results of 2-D simulations can be enriched when calibrated with the results of 3-D MD and DD simulations. Several groups performed 3-D discrete dislocation dynamic simulations (DDD). For example, Tang et al.[40] argued that the escape of mobile dislocations in smaller samples occurs faster than in larger ones, thereby demonstrating the reduction in mobile dislocation density, leading to greater resistance to plastic flow in smaller samples. On the other hand, Parthasarathy et al.[41] concluded that the observed size effects in 1–20 μm diameter micro-pillars are based on the statistical variation in the dislocation source lengths as revealed by simulations via ParaDis code.

Unfortunately, most DD simulations intentionally introduce initial dislocation pinning points, or Frank–Read sources, into the crystal, which inevitably causes dislocation multiplication, rendering dislocation starvation impossible to attain since these sources are not mobile. Very different results were obtained by Espinosa et al.[40,42] who incorporated jogged "single-arm" sources into a nanopillar using their 3-D PARANOID DDD code and discovered that not only the mobile dislocations but even the single-arm sources eventually leave the crystals after they carry plastic strain for some time in the simulation. This leads to a dislocation-starved state, consistent with nanopillar (<1 μm) experiments. More recently, Weygand et al.[43,44] performed 3-D simulations that accounted for traction free boundary conditions using the finite element method (FEM) and concluded that plasticity of small-scale samples is very sensitive to the underlying dislocation microstructure and is subject to statistical fluctuations. Due to the heavy calculations and difficult geometries needed to perform these simulations, detailed analyses were limited. To overcome such computational difficulties, El-Awady et al.[45] developed a self-consistent formulation of 3-D parametric dislocation dynamics (PDD) with the boundary element method (BEM) to incorporate the influence of free and internal interfaces on dislocation motion in order to describe micro-plastic flow in finite volumes. They performed large-scale simulations using this method and demonstrated that in contrast to 3-D models that ignore surface effects, image fields arising from the finite geometry of micro-pillars have an important effect on the dislocation microstructure, especially at the sub-micrometer dimensions.

This review clearly demonstrates a demand for an experimentally validated enrichment in the field that spans multiple length scales and microstructures. To accomplish this, several challenges remain in both computational and experimental approaches, with the main one being the lack of a direct comparison between them due to the discrepancies in the length and temporal scales. In this review, the attention is focused on the studying size effects arising during uniform deformation (i.e., tension and compression) because, at least in the case of single crystals, the material is not expected to strengthen through one of the known mechanisms like strain gradient plasticity, dislocation confinement, or initial lack of dislocations. This type of deformation also lends itself well to the calculation of stresses and strains, a much more powerful piece of information compared with load-displacement, for example. The demand for uncovering unique plasticity mechanisms operating in nano-scale volumes is imminent as the individual interactions between various types of defects have significant consequences on the materials' structural integrity, failure predictions, and ability to withstand harsh environments.

SAMPLE FABRICATION

Focused Ion Beam Approach

In the last decade or so, the FIB has become one of the most widely used tools for sample fabrication, testing, and imaging. This multidisciplinary tool is applicable to a broad range of projects like fabrication and testing of microelectromechanical systems (MEMS), nanoelectromechanical systems (NEMS), sensors, microactuators, and optoelectronic devices. The FIB can be utilized in the fabrication and analysis of intricate 3-D structures by both etching of the starting material and deposition of metals from gas phase. Figure 2 shows some of the representative mechanical testing specimens fabricated in our lab by using FEI Nova 200 Nanolab instrument with FIB at 30kV/10pA as the final etching condition: a free-standing nanocrystalline

nickel cylindrical nanopillar (Figure 2a), a single-crystalline 200-nm niobium tension sample (Figure 2b), and a single-crystalline molybdenum "hollow" pillar with cross section shown in inset (Figure 2c). To ensure homogeneous deformation, we intentionally maintain the aspect ratio (height/diameter) of the compression pillars at 4~5 and the tensile sample heights vary between 3 and 5 μm regardless of the diameter to ensure proper gripping.

Electron-beam Lithography and Electroplating Approach

Although the FIB-based nanomachining technique is capable of successful fabrication of microcompression and tension specimens, it has three distinct disadvantages: first, the minimum realistically attainable pillar diameter is ~150 nm, second, the degree to which ion bombardment on the surface structure translates to nanopillar mechanical performance remains a point of contention, and finally, it requires a large amount of time to manufacture individual samples, which significantly reduces the throughput. Therefore, we developed a nanomechanical sample fabrication methodology that does not utilize the damaging ion bombardment by using electron-beam lithography (EBL), and whose capability to produce small circular features on the order of 10 nm has been well documented. Electron-beam lithography is a top-down lithographic fabrication technique that employs a focused beam of high-energy electrons to expose a poly(methyl methacrylate) (PMMA) resist. The interaction of the electrons within PMMA solubilizes the exposed regions by severing chemical bonds and, after developing the resist in a chemical bath, the desired pattern is transferred onto the underlying seed metal film to enable further processing. Following the work of Mallouk et al.[46] we then deposit various metals within the open pores templated by EBL via electrochemical deposition where a metal ion salt solution is potentiostatically or galvanostatically reduced at the film surface, thus plating the desired metal. The specific fabrication details can be found in Reference 46. Figure 3 shows (a) a schematic of the fabrication procedure, (b) an array of nanocrystalline gold nanopillars, (c) a twinned candy-cane-like microstructure of a copper nanopillar, (d) an array of single-crystalline copper nanopillars with intentional overplates for tensile testing, and (e) a TEM image revealing the single-crystalline microstructure and close-to-<111> crystallographic orientation. Mechanical testing results indicate that these nanopillars exhibit a size effect virtually identical to the FIB'd pillars and will be reported in a separate manuscript.[47]

In-situ Mechanical Testing

For the mechanical testing experiments we utilize a custom-built piece of equipment, SEMentor, composed of two individual instruments: SEM and the nanoindenter, shown in Figure 4. The latter offers a precise control and high resolution of load and displacement (and their rates) as well as of contact stiffness during the experiment while the former allows for visualization of the process. We also fabricated tensile grips out of the standard indenter tip in a configuration that allows performing both tension and compression testing with the same tip (inset in Figure 4). This technique allows us to correlate the macroscopic stress–strain behavior with the microstructural changes taking place during the deformation by direct observation of the evolving surface morphology like slip lines and strain localization. In addition to the SEMentor experiments, we also perform the uniaxial compression experiments in the Nanoindenter G200 (Agilent Technologies) with a custom-made flat punch

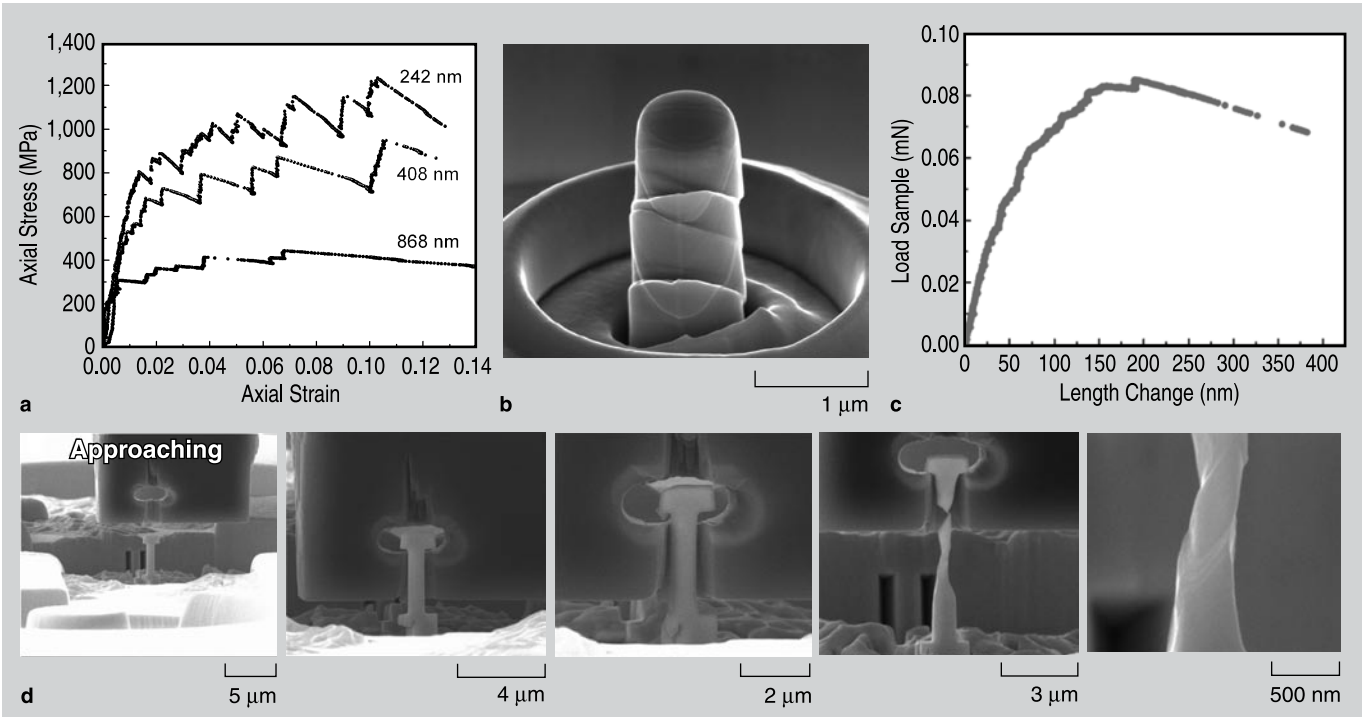

Figure 5. (a) Representative stress–strain curves of niobium nanopillars with different diameters clearly showing the stochastic nature of plasticity at the nano-scale even in b.c.c. metals. (b) Post-compression niobium nanopillar with pronounced slip offsets. (c) Load-displacement curve for a tension test of <001>-oriented gold sample. (d) Sequence of images during the tensile test.

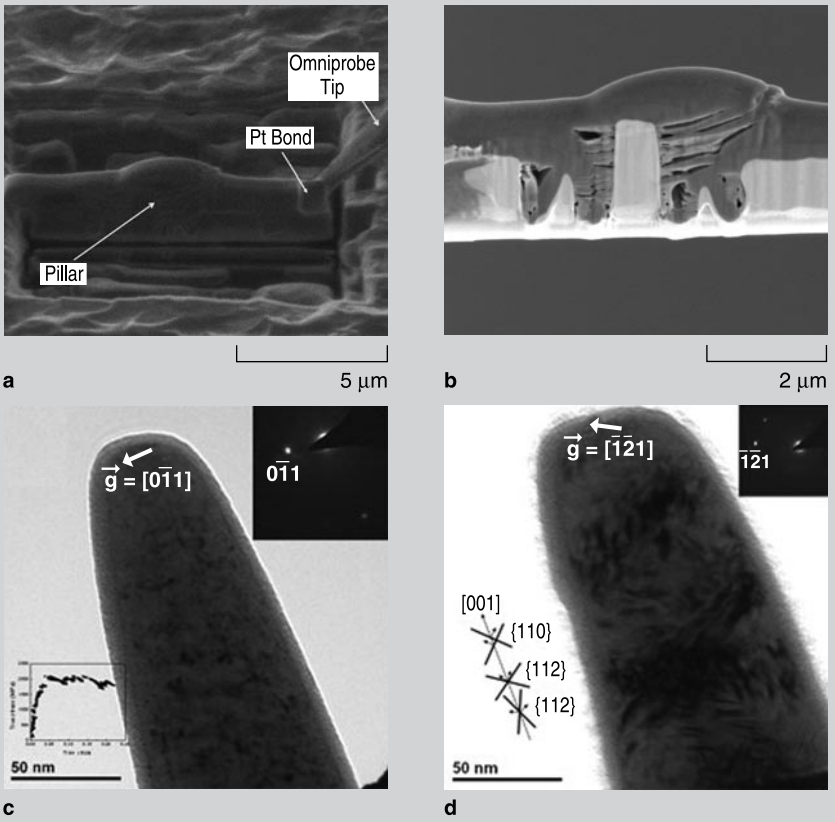

Figure 6. (a) Transmission electron microscopy lamella with platinum-coated pillar on top attached to the Omniprobe prior to severing the final attachment to the "parent" sample. (b) Same lamella after FIB thinning on TEM grid clearly revealing the pillar cross section. A TEM image of (c) undeformed and (d) deformed 100 nm-diameter niobium nanopillar compressed directly on TEM grid in SEMentor and revealing the formation of an intricate dislocation structure with multiple slip planes activated. Images from Reference 51.

indenter tip. To eliminate the additional complexity of strain rate effects within a single material class, all tests were performed at a constant nominal displacement rate (0.5 to 8 nm s^{-1}) controlled by a custom-written feedback-loop algorithm, resulting in nominal strain rates between 1.0×10^{-4} and 1.0×10^{-3} s^{-1}. Specimen-only response is isolated from the load frame, the support spring, and the substrate compliances, and stresses and strains are calculated based on the raw load-displacement data and the initial sample geometry as described in detail in Reference 21.

Size-dependent Strength as a Function of Microstructure

With the unique nanoscale fabrication and mechanical testing capabilities, we have been actively involved in studying plasticity in single crystals, specifically in b.c.c. structures like Mo, Nb, Ta, and W since their deformation appears to be more complex than that in f.c.c. crystals like Au. Several representative stress–strain curves of niobium nanopillars with different diameters clearly show the stochastic nature of plasticity at the nanoscale even in b.c.c. metals (Figure 5a). The image in Figure 5b shows a post-compression niobium nanopillar with pronounced slip offsets, while Figure 5c,d shows the load-displacement curve as well as a sequence of images during tensile testing of a gold nanopillar. The slip contours correspond to the locations of dislocation avalanches exiting the crystal at the free surfaces, as evidenced by the correlation between the discrete burst-like segments in the load-displacement curve and the formation of slip lines during the in situ experiments.

We find that both types of crystals, f.c.c. and b.c.c., exhibit a strong size effect, with the former significantly more pronounced than in all but niobium b.c.c. metals over the same diameter range.[17] The proposed hypothesis explaining this discrepancy is that it is due to the presence of the Peierls stress in b.c.c. metals and to the fundamental differences in dislocation behavior between the two types of crystals, as also suggested by atomistic simulations.[18] The free surfaces in nanopillars impose an additional so-called image force on the mobile dislocations, facilitating their transport toward the surface in f.c.c. crystals. In order for plasticity to commence, additional dislocations need to be nucleated, which requires the application of significantly higher stresses. To the contrary, the screw dislocations in b.c.c. crystals, which control their plasticity during mechanical loading, are likely to cross-slip, often exhibiting non-Schmid behavior, and travel in other, distinct crystallographic planes, leading to a greater chance of interacting with other dislocation segments and with themselves, thus forming forest-hardening-like network inside the crystal. This suggests that in b.c.c. pillars plasticity does not occur via dislocation starvation at the diameters we are studying, 100–900 nm. Interestingly, while the strength vs. size power law slope is –0.6 for most f.c.c. metals,[48] these slopes are different within the b.c.c. family: –0.93 for Nb, which is closer to that of Au (–0.9) rather than to Mo, W, and Ta (–0.4).[49] Furthermore, in studying the response of these crystals to different loading conditions (tension vs. compression), we find that while the attained stresses are equivalent for gold, there is a pronounced tension–compression asymmetry in all b.c.c. metals, especially in molybdenum.[49] Transmission electron microscopy analysis and atomistic simulations are underway to try to understand the link between dislocation behavior inside the pillars and the observed mechanical properties.

TEM MICROSTRUCTURAL ANALYSIS

We examine post-testing pillar microstructure evolved as a result of the imposed deformation via transmission electron microscopy (TEM, FEI Tecnai F30). Site-specific TEM sample preparation at this scale is impossible to accomplish with the conventional technique due to the less-than-1-µm pillar sizes. For these cases, we rely on the Omniprobe micromanipulator assisted site-specific sample preparation as described in detail in Reference 46. Subsequently, the lamella is transferred onto the TEM grid by bonding one of its sides to the grid with platinum, lo-

cally deposited via chemical vapor deposition from a gas-injection source, and severing the lamella's connection to the needle on the opposite side. Once the lamella with the sample of interest on top is securely attached to the grid, the structure is thinned down to an electron-transparent thickness[50] (Figure 6).

The major drawback of this technique is the inevitable sample damage introduced by Ga^+ during the thinning process, which affects the material surface by creating large numbers of FIB-induced dislocation loops and possibly implanted gallium. To avoid the damage induced by the thinning process, the 100-nm-diameter pillars were fabricated and compressed directly on the lamella, thereby not requiring any additional thinning after the deformation. This technique allows us to analyze the microstructure of the same pillar before (Figure 6c) and after (Figure 6d) the deformation, ensuring that any changes observed in the post-mortem pillar were a result of the deformation process and not of any sample preparation artifact.

CONCLUSION

This review conveys some of the recent advances in studying uniaxial deformation of small-scale metals and clearly shows that their mechanical properties, which determine the integrity and functionality of the structures they comprise, significantly depend on their size and initial microstructure. Focused ion beam-fabricated single-crystalline f.c.c. nanopillars tend to exhibit a unified power-law size dependence with the exponent of ~ –0.6 independent of orientation, rate control, and loading path. On the other hand, b.c.c. metals show less pronounced increase in strength with reduced size and additional variation in the slope correlated with the remaining effects of the Peierls stress at room temperature. Furthermore, while f.c.c. nanoscale metals attain equivalent stresses in compression and tension, b.c.c. metals exhibit non-trivial tension-compression asymmetry, which is a function of the specific metal, its crystallographic orientation, and strain rate. The key difference between these findings and those based on the deformation of metallic nanopillars made by most non-FIB-based fabrication techniques is that the latter generally have a pristine microstructure, with no initial dislocations, and, not surprisingly, attain nearly theoretical strengths during deformation. Our most recent findings on the compression and tension of FIB-lessly produced single crystalline copper nanopillars yet with non-zero initial dislocation densities reveal an identical size effect to the FIB-fabricated ones, thereby validating the size effect as an intrinsic material property rather than an effect of a damaged layer. While these and other prominent advances in nano-scale mechanics provide a solid foundation for understanding defect evolution, and therefore, material properties at small scales, a greater challenge of connecting the nanoscale deformation mechanisms with the macro-scale material properties remains. A fundamental understanding of these issues will be key in the synthesis and development of multifunctional, reliable materials.

ACKNOWLEDGEMENTS

The authors gratefully acknowledge financial support from the National Science Foundation CAREER Award (DMR-0748267) and ONR Grant# N000140910883 as well as Kavli Nanoscience Institute (KNI) cleanroom facility at Caltech. We also thank R. Groger, V. Gavini, W.L. Johnson, and C.A. Schuh for insightful discussions and for bulk samples.

References

1. W.D. Nix et al., *Thin Solid Films,* 515 (2007), p. 3152.
2. C.V. Thompson, *J. Materials Research,* 8 (1993), p. 237.
3. B. von Blanckenhagen, P. Gumbsch, and E. Arzt, *Philosophical Magazine Letters,* 83 (2003), p. 1.
4. M.S. De Guzman, *Materials Research Society Symposium Proceedings 308* (Warrendale, PA: Materials Research Society, 1993), p. 613.
5. N.A. Fleck et al., *Acta Materialia,* 42 (1994), p. 475.
6. N.A. Fleck and J.W. Hutchinson, *J. Mechanics and Physics of Solids,* 49 (2001), p. 2245.
7. H. Gao et al., *J. Mechanics and Physics of Solids,* 47 (1999), p. 1239.
8. G. Yun et al., *Philosophical Magazine,* 86 (2006), p. 5553.
9. A. Acharya, *J. Mechanics and Physics of Solids,* 49 (2001), p. 761.
10. A. Acharya, *J. Mechanics and Physics of Solids,* 52 (2004), p. 301.
11. M.E. Gurtin, *J. Mechanics and Physics of Solids,* 50 (2002), p. 5.
12. M.D. Uchic et al., *Science,* 305 (2004), p. 986.
13. D.M. Dimiduk, M.D. Uchic, and T.A. Parthasarathy, *Acta Materialia,* 53 (2005), p. 4065.
14. Z.W. Shan et al., *Nature Materials* (2008), p. 7.
15. J.R. Greer et al., *Acta Materialia,* 53 (2005), p. 1821.
16. J.R. Greer and W.D. Nix, *Physical Review B,* 73 (2006), 245410.
17. C.A. Volkert and E.T. Lilleodden, *Philosophical Magazine,* 86 (2006), p. 5567.
18. A. Budiman et al., *Acta Materialia,* 56 (2007), p. 602.
19. D. Kiener et al., *Materials Science and Engineering A,* 459 (2006), p. 262.
20. H. Bei, E.P. George, and G.M. Pharr, *Materials Science and Engineering A,* 483-484 (2008), p. 218.
21. J.-Y. Kim and J.R. Greer, *Applied Physics Letters* (2008), p. 93.
22. K.S. Ng and A.H.W. Ngan, *Scripta Materialia,* 59 (2008), p. 796.
23. S. Brinckmann, J.-Y. Kim, and J.R. Greer, *Physical Review Letters,* 100 (2008), 155502.
24. C.A. Volkert et al., *Applied Physics Letters,* 89 (2006), 061920.
25. D. Kiener et al., *Acta Materialia,* 56 (2008), p. 580.
26. S.H. Oh et al., *Nature Materials* (2009), p. 8.
27. G. Dehm, *Progress in Materials Science,* 54 (2009), p. 664.
28. D. Kiener, W. Grosinger, and G. Dehm, *Scripta Materialia,* 60 (2009), p. 148.
29. D. Kiener, C. Motz, and G. Dehm, *Materials Science and Engineering A,* 505 (2009), p. 79.
30. J.-Y. Kim and J.R. Greer, *Acta Materialia,* 57 (2009), p. 5245.
31. S.S. Brenner, *J. Applied Physics* (1956), p. 27.
32. G. Richter et al., *Nano Letters* (2009), doi: 10.1021/nl9015107.
33. H. Bei et al., *Acta Materialia* (2008), p. 56.
34. S. Lee, S. Han, and W.D. Nix, *Acta Materialia,* 57 (2009), p. 4404.
35. J.R. Greer, C. Weinberger, and W. Cai, *Materials Science and Engineering A,* 493 (2008), p. 21.
36. C. Weinberger and W. Cai, *Proceedings of the National Academy of Sciences of the USA,* 105 (2008), p. 14304.
37. V.S. Deshpande, A. Needleman, and E. Van der Giessen, *J. Mechanics and Physics of Solids,* 53 (2005), p. 2661.
38. A.A. Benzerga and N.F. Shaver, *Scripta Materialia,* 54 (2006), p. 1937.
39. P.J. Guruprasad and A.A. Benzerga, *J. Mechanics and Physics of Solids,* 56 (2008), p. 132.
40. H. Tang, K.W. Schwartz, and H.D. Espinosa, *Acta Materialia,* 55 (2007), p. 1607.
41. T.A. Parthasarathy et al., *Scripta Materialia,* 56 (2007), p. 313.
42. H.D. Espinosa et al., *Int'l. Jrnl. Plasticity,* 22 (2006), p. 2091.
43. D. Weygand et al., *Materials Science and Engineering A,* 483-484 (2008), p. 188.
44. J. Senger et al., *Scripta Materialia,* 58 (2008), p. 587.
45. J.A. El-Awady, S.B. Biner, and N.M. Ghoniem, *J. Mechanics and Physics of Solids,* 56 (2008), p. 2019.
46. M.J. Burek and J.R. Greer, *Nano Letters* (2009), submitted.
47. A.T. Jennings, M.J. Burek, J.R. Greer, *Proc. Nat. Acad. Sciences* (2009), p. 2880–2886.
48. R. Dou and B.A. Derby, *Scripta Materialia,* 61 (2009), p. 524.
49. J.-Y. Kim and J.R. Greer, *Acta Materialia* (2009), submitted.
50. J.R. Greer et al., *Advanced Functional Materials* (2009), p. 19.
51. J.-Y. Kim, D. Jang, and J.R. Greer, *Scripta Materialia,* 61 (2009), p. 300.

Julia R. Greer, assistant professor of materials science and mechanics, and Ju-Young Kim, postdoctoral scholar, are with the California Institute of Technology, Pasadena, CA 91125; Michael J. Burek is a student at the University of Waterloo, Waterloo, Canada. Prof. Greer can be reached at jrgreer@caltech.edu.